Salinity, oxygen isotope, hydrogen isotope, and radiocarbon of coastal seawater of North Japan

Kubota, Kaoru ; Sakai, Keisuke ; Ohkushi, Ken'ichi ; Higuchi, Tomihiko ; Shirai, Kotaro ; Minami, Masayo

(Citation)
Geochemical Journal,56(6):240-249

(Issue Date)
2022-12-16

(Resource Type)
journal article

(Version)
Version of Record

(URL)
https://hdl.handle.net/20.500.14094/0100483243

GEOCHEMICAL JOURNAL THE GEOCHEMICAL SOCIETY OF JAPAN
DATA

Salinity, oxygen isotope, hydrogen isotope, and radiocarbon of coastal seawater of North Japan

Kaoru Kubota[1,2*], Keisuke Sakai[2], Ken'ichi Ohkushi[2], Tomihiko Higuchi[3], Kotaro Shirai[3], and Masayo Minami[4]

[1] Research Institute for Marine Geodynamics, Japan Agency for Marine–Earth Science and Technology, 2-15 Natsushima, Yokosuka, Kanagawa 237-0061, Japan
[2] Graduate School of Human Development and Environment, Kobe University, 3-11 Tsurukabuto, Nada-ku, Kobe, Hyogo 657-8501, Japan
[3] Atmosphere and Ocean Research Institute, The University of Tokyo, 5-1-5 Kashiwanoha, Kashiwa, Chiba 277-8564, Japan
[4] Institute for Space–Earth Environmental Research, Nagoya University, Furo-cho, Chikusa-ku, Nagoya, Aichi 464-8601, Japan

* Corresponding author E-mail: kaoryu0129@gmail.com

Abstract To understand seawater properties, such as water mass structure and mixing, geochemical analyses are useful. However, geochemical datasets for seawater that fully cover coastal areas of Hokkaido, North Japan are lacking. Here we report comprehensive geochemical analyses of seawater (salinity, $\delta^{18}O$, δD, and $\Delta^{14}C$) collected in August–September 2021 from coastal areas of Hokkaido as well as the west coast of Tohoku (Northeast Japan). These datasets are expected to improve our understanding of seawater properties around Hokkaido, thereby contributing to oceanography, climatology, biogeochemical cycles, and fishery science.

Keywords oxygen isotope, hydrogen isotope, radiocarbon, salinity, Hokkaido

Dates Received: August 5, 2022 Accepted: November 26, 2022 Advance publication: December 16, 2022

Introduction

Geochemical analyses of seawater provide important insight into water properties such as water mass structure and mixing. Around Hokkaido, the Tsushima Warm Current originating from the Kuroshio Current flows northward over the Japan Sea, and after passing through the Soya Strait, it changes into the Soya Warm Current and flows eastward along the coast (Fig. 1). On the southern coast of Hokkaido, the Oyashio Current originating from the North Pacific Ocean flows westward along the coast and collides and mixes with the Tsugaru Warm Current (the Tsushima Warm Current after passing through the Tsugaru Strait) (Fig. 1). However, this is only a rough illustration of the ocean current system, and there is substantial, highly complex variation on long and short time scales. A better understanding of seawater properties around Hokkaido is needed for applications in oceanography, climatology, biogeochemical cycles, and fishery science.

Among measurable parameters of seawater, salinity and oxygen and hydrogen stable isotopes ($\delta^{18}O$ and δD) can be analyzed relatively easily and thus are widely used as water mass proxies.

In tandem with temperature, salinity is a fundamental indicator of seawater properties. Specifically, T-S diagrams and salinity are used to detect the mixing of different water masses and the evaporation/precipitation balance (Kodaira *et al.*, 2016). In coastal areas, salinity can reveal mixing between seawater and freshwater (river water, groundwater, etc.) (Kubota *et al.*, 2018a).

Similar to salinity, $\delta^{18}O$ and δD are important parameters to characterize seawater properties such as water mass difference (Voelker *et al.*, 2015; LeGrande and Schmidt, 2006). Also, they are particularly powerful tracers in coastal environments (e.g., estuary, delta,

Citation Kubota, K., Sakai, K., Ohkushi, K., Higuchi, T., Shirai, K. and Minami, M. (2022) Salinity, oxygen isotope, hydrogen isotope, and radiocarbon of coastal seawater of North Japan. *Geochem. J.*, **56**, 240–249.

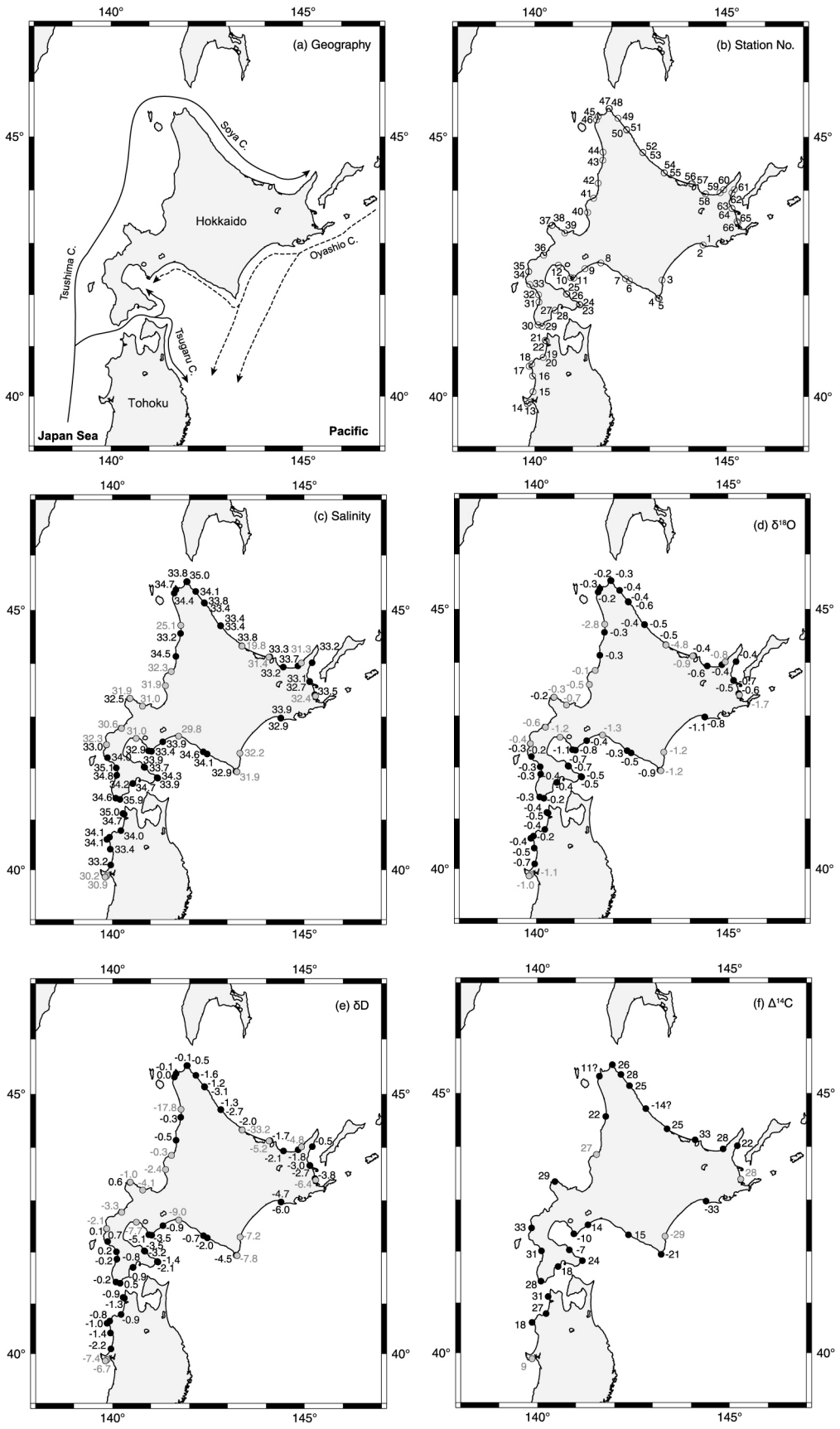

Fig. 1. Geographic map of the study area and results of a geochemical analysis of coastal seawater of Hokkaido and the west coast of North Japan. (a) Geography of the study area with major water current systems (solid line with arrows: warm currents, dashed lines with arrows: cold currents). (b) Locations of seawater sampling points with site numbers (Site No. 1–12 were visited August 20–22, 2021 and site No. 13–66 were visited September 7–16, 2021). Analyses of (c) salinity, (d) $\delta^{18}O$, (e) δD, and (f) $\Delta^{14}C$. Black/gray circles indicate cases with salinity higher/lower than 32.5 psu.

watershed), because isotopic compositions are distinctly different between seawater and freshwater (Nair *et al.*, 2015; Carreira *et al.*, 2014). In particular, the oxygen isotope ratio of calcium carbonate ($CaCO_3$) skeletons and shells biogenically precipitated in seawater is widely used as a thermometer, as isotopic fractionation is dependent on temperature (note that this applies only when the oxygen isotopic ratio of seawater [$\delta^{18}O_{SW}$] does not vary with time or can be estimated) (Kubota *et al.*, 2015, 2017; Suzuki *et al.*, 2005; Schöne *et al.*, 2004; McConnaughey, 1989; Grossman and Ku, 1986). Conversely, when temperature is reconstructed by an independent method (e.g., Sr/Ca thermometers based on coral skeletons and Mg/Ca thermometers based on foraminifera shells), past $\delta^{18}O_{SW}$ can be quantitatively reconstructed, enabling the reconstruction of the evaporation/precipitation balance (and hence dry/wet conditions) in the surface ocean. This has been demonstrated using long-living coral skeletons (e.g., Cahyarini *et al.*, 2014; Felis *et al.*, 2009) and foraminifera shells preserved in marine sediment (Mohtadi *et al.*, 2010; de Garidel-Thoron *et al.*, 2007).

In addition, radiocarbon ($\Delta^{14}C$) is a powerful tracer in seawater (Broecker *et al.*, 1985). $\Delta^{14}C$ is a widely used tracer in a broad range of fields, including oceanography and fishery science (Ota *et al.*, 2019; Larsen *et al.*, 2018; Hirabayashi *et al.*, 2017; Mitsuguchi *et al.*, 2016; Kumamoto *et al.*, 2013; Tsunogai *et al.*, 1995). In the modern ocean, anthropogenic radiocarbon invades the natural carbon cycles (Östlund and Stuiver, 1980). Anthropogenic radiocarbon, bomb-^{14}C, is a biproduct of atmospheric thermonuclear bomb testing in the 1950s and 1960s (the high-energy neutrons produced by the bombs fused with atmospheric ^{14}N to produce ^{14}C). After the Partial Test Ban Treaty (PTBT) became effective in 1963, new bomb-^{14}C input ceased, but modern surface seawater is still being contaminated with bomb-^{14}C. $\Delta^{14}C$ in the surface seawater decreases by natural carbon cycle dynamics (i.e., the absorption of carbon by ocean and terrestrial ecosystems) and by dilution by anthropogenic carbon emissions, such as the combustion of fossil fuels in which ^{14}C is totally decayed (^{14}C Suess effect; Suess, 1953). In summary, $\Delta^{14}C$ of the surface seawater changes over time and ideally needs to be reconstructed continuously. $\Delta^{14}C$ measurements at offshore sites using research vessels are available (e.g., GLODAP: Global Ocean Data Analysis Project, Olsen *et al.*, 2016); however, shipboard measurements provide only a snapshot of $\Delta^{14}C$ and do not sufficiently capture the substantial spatiotemporal variability. In addition, it is quite difficult to obtain a continuous bomb-^{14}C record, especially in high-latitude oceans lacking long-living reef-building coral skeleton made of calcium carbonate ($CaCO_3$), suitable for generating a detailed record. In Japan, the northern limit of the reef-building coral distribution is Iki Island, West Japan (33°47'N, 129°43'E) (Yamano *et al.*, 2001), and this area has been the northern limit of the bomb-^{14}C record around Japan (Mitsuguchi *et al.*, 2016). Kubota *et al.* (2018b, 2021) reported the first quasi-continuous seawater bomb-^{14}C record of a relatively high-latitude coastal region, the Otsuchi area of the Pacific side of Tohoku (39°23'N, 141°57'E), using several long-living bivalve shells made of $CaCO_3$ (*Mercenaria stimpsoni*). As *M. stimpsoni* is widely distributed around North Japan, including all coastal areas of Hokkaido and the west coast of Tohoku (the Japan Sea side), it may be possible to establish a bomb-^{14}C record based on shells at various sites in North Japan. To the best of our knowledge, there are no reports of $\Delta^{14}C$ of modern seawater on the west coast of Tohoku or in coastal areas of Hokkaido, and there are only limited reports of $\Delta^{14}C$ of mollusk shells in the pre-bomb era (before 1950) (Kuzmin *et al.*, 2001, 2007; Yoneda *et al.*, 2000, 2007), used for ^{14}C marine reservoir age estimation from ^{14}C records.

Here we report a comprehensive geochemical dataset of seawater parameters (salinity, $\delta^{18}O$, δD, and $\Delta^{14}C$) collected in August–September 2021 from shallow water (<10 m) of all coastal areas around Hokkaido as well as the west coast of Tohoku. As the first such dataset for the region, these results have important implications for our understanding of modern properties of coastal water in the area and provide a basis for various practical applications.

Materials and Methods

Seawater was collected from all coastal areas around Hokkaido as well as the west coast of Tohoku during two field surveys during August 20–22, 2021 and September 7–16, 2021 (**Fig. 1**). Water samples were collected in two ways (Type A and B). In Type A sampling (for salinity, $\delta^{18}O$, and δD analyses), water samples were collected at beaches (water depth less than 0.3 m, **Table 1**). In type B sampling (for salinity, $\delta^{18}O$, δD, and radiocarbon analyses), a stainless-steel water sampler with a long rope and a 500 mL grass bottle (Sibata, Sōka, Japan) was used from wharves (water depth 0.5–10 m, **Table 1**), and the 500 mL water samples were divided into storage bottles according to measurement purposes. For all samples, water temperature, conductivity, and pH were measured just after sample collection by using a portable water quality analyzer (LAQUA D-200 series; Horiba, Kyoto, Japan). The dissolved oxygen (DO) concentration was measured by using a portable oxygen meter (DO–5510 HA; Lutron, Coopersburg, PA). The weather at the time of sampling was sunny in most cases, with occasional cloudy days and one rainy day on August 22, 2021 (**Table 1**).

All water samples were filtered at the water collection sites through a 0.45-μm Millipore PTFE membrane

Table 1. Results of a geochemical analysis of coastal seawater of Hokkaido and the west coast of Tohoku

Site No.	Date	Weather	Longitude	Latitude	Water Depth (m)	Sampling Type	pH	Conductivity (mS/cm)	DO (mg/L)	Water Temperature (°C)	Salinity (psu)	$\Delta^{14}C$ (‰)	$\Delta^{14}C$_stdev	$\delta^{18}O$ (‰)	$\delta^{18}O$_stdev	δD (‰)	δD_stdev	Remark
1	2021/8/20	Sunny	144.3878	42.9675	3.5	B	7.62	51.7	6.6	19.3	33.9	–41	5	–0.8	0.2	–4.7	0.7	
2	2021/8/20	Sunny	144.3892	42.9689	0.3	A	7.89	50.9	10.1	21.6	32.9			–1.1	0.2	–6.0	0.6	
3	2021/8/20	Sunny	143.3214	42.2950	7.5	B	7.80	49.7	15.9	17.8	32.2	–37	5	–1.2	0.1	–7.2	0.3	
4	2021/8/21	Sunny	143.2183	41.9464	1.5	B	8.00	49.2	13.5	20.3	32.9	–30	5	–0.9	0.2	–4.5	0.6	
5	2021/8/21	Cloudy	143.2442	41.9331	0.2	A	8.32	49.4	14.2	19.6	31.9			–1.2	0.1	–7.8	0.4	
6	2021/8/21	Sunny	142.4692	42.2808	0.3	A	8.40	49.8	9.2	29.1	34.1			–0.5	0.1	–2.0	0.6	
7	2021/8/21	Sunny	142.3678	42.3233	3.5	B	8.11	50.9	10.7	22.3	34.6	7	5	–0.3	0.2	–0.7	0.5	
8	2021/8/21	Sunny	141.7272	42.6253	0.2	A	8.10	45.8	10.7	25.4	29.8			–1.3	0.1	–9.0	0.6	
9	2021/8/21	Sunny	141.3111	42.5153	10.0	B	7.88	51.3	14.5	21.3	33.9	5	5	–0.4	0.3	–0.9	0.5	
10	2021/8/22	Rainy	140.9425	42.3417	1.6	B	7.84	47.2	8.8	21.1	32.9	–18	5	–1.1	0.0	–5.1	0.3	
11	2021/8/22	Rainy/Cloudy	141.0228	42.3314	0.1	A	7.89	48.1	4.4	21.2	33.4			–0.8	0.1	–3.5	0.4	
12	2021/8/22	Rainy	140.6203	42.5794	0.0	A	7.97	46.8	8.6	22.5	31.0			–1.2	0.1	–7.7	0.7	
13	2021/9/7	Sunny	139.8589	39.8856	1.3	B	7.95	46.0	5.9	25.8	30.2	0	5	–1.1	0.2	–7.4	0.9	
14	2021/9/7	Sunny	139.8158	39.8572	0.3	A	8.31	46.0	7.1	28	30.9			–1.0	0.1	–6.7	0.6	
15	2021/9/7	Sunny	139.9592	40.0981	0.1	A	8.17	50.7	8.8	26.9	33.2			–0.7	0.1	–2.2	0.5	
16	2021/9/7	Sunny	139.9481	40.4133	0.2	A	8.26	51.0	8.8	25.5	33.4			–0.5	0.1	–1.4	0.5	
17	2021/9/7	Sunny	139.8611	40.6081	2.0	B	8.10	50.5	5.5	24.9	34.1	9	5	–0.4	0.0	–1.0	0.4	
18	2021/9/8	Cloudy	139.9283	40.6536	0.2	A	7.78	52.0	9.1	21.4	34.1			–0.2	0.1	–0.8	0.3	
19	2021/9/8	Cloudy	140.2233	40.7811	0.5	B	8.11	50.9	9	23.1	34.0	18	5	–0.4	0.0	–0.9	0.3	
20	2021/9/8	Cloudy	140.2236	40.7811	0.2	A	7.93	50.3	8.7	22.9								Sample lost
21	2021/9/8	Cloudy	140.2797	41.1203	3.6	B	7.99	51.0	4.8	22.8	35.0	22	5	–0.4	0.1	–0.9	0.1	
22	2021/9/8	Cloudy	140.3081	41.1025	0.3	A	8.13	50.9	8.9	22.8	34.7			–0.5	0.1	–1.3	0.5	
23	2021/9/9	Cloudy	141.1833	41.8131	0.3	A	7.78	52.1	6.2	22.7	33.9			–0.5	0.1	–1.4	0.2	
24	2021/9/9	Sunny	141.1689	41.8225	4.5	B	7.96	51.4	9.5	21.8	34.3	15	5	–0.5	0.1	–2.1	0.3	
25	2021/9/9	Sunny	140.8439	42.0214	0.0	A	7.98	50.7	9.7	23	33.7			–0.7	0.1	–3.2	0.5	
26	2021/9/9	Cloudy	140.8272	42.0322	2.1	B	7.78	51.3	9.4	23.1	33.9	–15	7	–0.7	0.1	–3.5	0.3	
27	2021/9/9	Sunny	140.5358	41.7083	2.9	B	8.06	51.8	8.1	24.2	34.2	9	7	–0.4	0.1	–0.8	0.2	
28	2021/9/9	Sunny	140.5339	41.7081	0.0	A	8.04	52.2	9.2	25.9	34.7			–0.4	0.2	–0.9	0.3	
29	2021/9/10	Sunny	140.1986	41.3978	0.2	A	7.86	53.5	9.6	25.3	35.9			–0.2	0.1	0.5	0.6	
30	2021/9/10	Sunny	140.0906	41.4211	4.0	B	7.89	52.8	10.2	24.7	34.6	19	7	–0.3	0.1	–0.2	0.3	
31	2021/9/10	Sunny	140.1156	41.8667	0.2	A	7.98	52.6	5.8	28.1	34.8			–0.3	0.0	–0.2	0.4	
32	2021/9/10	Sunny	140.1031	42.0100	1.6	B	7.97	52.1	10.1	25.5	35.1	22	7	–0.3	0.1	0.2	0.3	
33	2021/9/10	Sunny	139.8756	42.2117	0.0	A	7.99	52.0	10.4	27	34.0			–0.2	0.0	0.7	0.3	

Table 1. (continued)

Site No.	Date	Weather	Longitude	Latitude	Water Depth (m)	Sampling Type	pH	Conductivity (mS/cm)	DO (mg/L)	Water Temperature (°C)	Salinity (psu)	$\Delta^{14}C$ (‰)	$\Delta^{14}C$_stdev	$\delta^{18}O$ (‰)	$\delta^{18}O$_stdev	δD (‰)	δD_stdev	Remark
34	2021/9/10	Sunny	139.8492	42.4583	0.2	A	7.99	50.3	9.6	26.1	32.3			–0.4	0.1	–2.1	0.3	
35	2021/9/10	Sunny	139.8472	42.4522	3.2	B	7.93	52.4	9.9	24.5	33.0	24	7	–0.3	0.1	0.1	0.4	
36	2021/9/11	Sunny	140.2400	42.7756	0.2	A	7.99	47.4	8.2	25.2	30.6			–0.6	0.0	–3.3	0.5	
37	2021/9/11	Sunny	140.4533	43.3422	1.6	B	8.10	51.5	9.5	24.9	32.5	20	7	–0.2	0.0	0.6	0.3	
38	2021/9/11	Sunny	140.4608	43.3461	0.2	A	8.13	49.9	8.9	25.8	31.9			–0.3	0.1	–1.0	0.4	
39	2021/9/11	Sunny	140.7875	43.1992	0.1	A	8.18	48.5	8.1	27.9	31.0			–0.7	0.2	–4.1	0.4	
40	2021/9/13	Sunny	141.3853	43.5878	0.0	A	8.19	49.7	8.7	23	31.9			–0.5	0.0	–2.4	0.7	
41	2021/9/13	Cloudy	141.5331	43.8525	3.2	B	8.03	50.4	9.5	21.5	32.3	18	7	–0.1	0.1	–0.3	0.1	
42	2021/9/13	Sunny	141.6539	44.1372	0.0	A	8.00	50.2	8.9	22.2	34.5			–0.3	0.1	–0.5	0.5	
43	2021/9/13	Sunny	141.7744	44.5653	1.0	B	7.60	47.6	9.9	22.4	33.2	13	7	–0.3	0.1	–0.3	0.7	
44	2021/9/13	Sunny	141.7822	44.7156	0.1	A	7.69	36.5	9.7	20.4	25.1			–2.8	0.2	–17.8	0.6	
45	2021/9/13	Sunny	141.6553	45.3717	0.0	A	7.82	50.1	9.8	19.6	34.7			–0.3	0.1	–0.1	0.3	
46	2021/9/13	Sunny	141.6136	45.3097	3.4	B	7.80	49.8	9.3	19.5	34.4	2	7	–0.2	0.1	0.0	0.2	
47	2021/9/14	Sunny	141.9375	45.5225	0.2	A	7.92	50.5	10	21.1	33.8			–0.3	0.0	–0.5	0.1	
48	2021/9/14	Sunny	141.9461	45.5208	4.4	B	7.85	51.6	10.4	24.1	35.0	18	7	–0.2	0.1	–0.1	0.5	
49	2021/9/14	Sunny	142.1686	45.3411	2.5	B	7.46	49.6	5	21.4	34.1	19	7	–0.4	0.1	–1.6	0.2	
50	2021/9/14	Sunny	142.4017	45.1250	0.0	A	7.95	51.0	6.9	20.6	33.8			–0.4	0.0	–1.2	0.1	
51	2021/9/14	Sunny	142.3928	45.1336	2.0	B	7.94	48.6	8.9	21.2	33.4	16	7	–0.6	0.1	–3.1	0.5	
52	2021/9/15	Sunny	142.8161	44.7097	2.1	B	8.04	49.6	9.2	20.7	33.4	–23	7	–0.5	0.2	–2.7	0.4	
53	2021/9/15	Sunny	142.8183	44.7078	0.2	A	8.04	50.5	8.5	22.1	33.4			–0.4	0.1	–1.3	0.2	
54	2021/9/15	Sunny	143.3742	44.3358	6.0	B	8.07	49.6	8.9	21.3	33.8	16	7	–0.5	0.0	–2.0	0.7	
55	2021/9/15	Sunny	143.3783	44.3278	0.0	A	7.91	33.4	9.1	19	19.8			–4.8	0.0	–33.2	0.4	
56	2021/9/15	Sunny	144.0742	44.1236	0.0	A	8.08	47.8	9.7	21	31.4			–0.9	0.1	–5.2	0.3	
57	2021/9/15	Sunny	144.1011	44.1278	3.4	B	7.87	51.0	9.5	21	33.3	24	7	–0.4	0.1	–1.7	1.1	
58	2021/9/16	Sunny	144.4525	43.9350	0.0	A	7.77	49.0	9.2	18.9	33.2			–0.6	0.0	–2.1	0.1	
59	2021/9/16	Sunny	144.8347	43.9581	0.6	B	7.88	50.0	10.1	19.3	33.7	19	7	–0.4	0.1	–1.8	0.6	
60	2021/9/16	Sunny	144.9186	44.0133	0.0	A	7.97	48.9	6.7	20.9	31.3			–0.8	0.1	–4.8	0.5	
61	2021/9/16	Sunny	145.2006	44.0200	5.7	B	8.13	52.0	10.8	21.3	33.2	14	7	–0.4	0.1	–0.5	0.4	
62	2021/9/16	Sunny	145.1342	43.9550	0.0	A	8.05	48.0	10	21								Sample lost
63	2021/9/16	Sunny	145.1350	43.6653	4.4	B	7.75	50.6	10.2	20.4	33.1			–0.7	0.2	–2.7	0.6	
64	2021/9/16	Sunny	145.1367	43.6589	0.1	A	8.01	50.0	9.9	20.9	32.7			–0.5	0.1	–3.0	0.8	
65	2021/9/16	Sunny	145.2883	43.3886	3.0	B	7.83	49.9	10.9	18.3	32.4	19	7	–1.7	1.6	–6.4	3.2	
66	2021/9/16	Sunny	145.2711	43.4147	0.0	A	7.97	47.3	10.3	18.4	33.5			–0.6	0.0	–3.8	0.0	

Table 2. Average values, standard deviations, and count data for salinity, $\delta^{18}O$, δD, and $\Delta^{14}C$ for two water sampling methods—Type A (collection from shallow water at beaches) and Type B (collection from wharves)

All data	Sampling Type A				Sampling Type B			
	Salinity	$\delta^{18}O$	δD	$\Delta^{14}C$	Salinity	$\delta^{18}O$	δD	$\Delta^{14}C$
Average	32.4	–0.78	–4.10		33.5	–0.53	–2.07	6.3
Standard deviation	3.0	0.87	6.25		1.0	0.35	2.24	19.0
Count	34	34	34		30	30	30	29
Data with high salinity (>32.5)	**Sampling Type A**				**Sampling Type B**			
	Salinity	$\delta^{18}O$	δD	$\Delta^{14}C$	Salinity	$\delta^{18}O$	δD	$\Delta^{14}C$
Average	33.9	–0.48	–1.63		33.8	–0.45	–1.57	7.1
Standard deviation	0.8	0.23	1.60		0.7	0.21	1.59	17.8
Count	21	21	21		26	26	26	26

Units are psu for salinity and permil for $\delta^{18}O$, δD, and $\Delta^{14}C$.

(Merck Millipore, Billerica, MA) using a filtration device equipped with a hand vacuum pump. For salinity, $\delta^{18}O$, and δD analyses, the samples were stored in 250 mL PP bottles (AsOne, Osaka, Japan) without headspace. These samples were refrigerated until analysis in a laboratory. For the radiocarbon analysis, samples were stored in 250 mL PAN (acrylonitrile butadiene methyl acrylate) bottles with a high-performance gas barrier (Nikko Hansen, Osaka, Japan), which enables long-term storage of water samples without contaminating modern carbon (Takahashi *et al.*, 2019). The samples were shipped to the laboratory at Nagoya University and ^{14}C in seawater dissolved inorganic carbon (DIC) was quickly analyzed using a headspace method (described later).

In a laboratory of Kobe University, salinity of the samples was measured using a portable salinity meter (LAQUA act; Horiba) calibrated with standard solutions. The measurements were conducted over two consecutive days (October 21–22, 2021). The salinity estimates of IAPSO standard seawater (Batch: P153; OSIL, Havant, United Kingdom; certified salinity of 34.994 psu; Bacon *et al.*, 2007) were 33.1 and 34.3 psu on October 21, 2021 and October 22, 2021, respectively. These values were used as a calibration coefficient for each day.

After measuring salinity, the remaining water samples stored in PP bottles were shipped to the Atmosphere and Ocean Research Institute, The University of Tokyo, for $\delta^{18}O$ and δD measurements using a wavelength-scanned cavity ring-down spectroscopy isotopic water analyzer (L2120-i; Picarro, Santa Clara, CA). Repeated analyses of Milli-Q water yielded values of –9.71 ± 0.06‰ (1 standard deviation [SD]) for $\delta^{18}O$ and –65.44 ± 0.51‰ for δD. These standard deviations were used as the analytical uncertainty for isotopic measurements. Isotopic values of water samples are reported relative to Vienna Standard Mean Ocean Water (VSMOW).

The ^{14}C in DIC was determined by a headspace method (Takahashi *et al.*, 2021). Briefly, CO_2 was extracted from seawater into the headspace of the reaction container. Then, CO_2 was introduced into the vacuum line by gas expansion and cryogenically purified using an ethanol-slush trap (ca. –100°C). The purified CO_2 was converted to graphite by a Fe catalyst at 620°C for 6 h. The target graphite samples were measured with a Tandetron accelerator mass spectrometer (AMS; High Voltage Engineering Europa, Amersfoort, the Netherlands) installed at the Institute for Space–Earth Environmental Research, Nagoya University. Results are reported according to the standardized system proposed by Stuiver and Polach (1977). Data were corrected for mass fractionation using the $\delta^{13}C$ value and are presented as $\Delta^{14}C$ in which years of formation were set to the year of collection, 2021. The error of the $\Delta^{14}C$ analysis at Nagoya University was smaller than 8‰ (**Table 1**).

Results

We report geochemical datasets for 66 sites. Note that Type A sampling and Type B sampling were often conducted at the same locations (**Fig. 1**, **Table 1**). The sampling distribution depended on whether each method was possible at the site. At two sites (Site Nos. 20 & 62), collected water samples were measured *in situ* and were later lost during transport. Water temperature, salinity, pH, conductivity, DO, $\delta^{18}O$, δD, and $\Delta^{14}C$ values for the samples ranged from 17.8°C to 29.1°C (samples may have warmed after collection), 19.8 to 35.9 psu, 7.46 to 8.40, 33.4 to 53.5 mS/cm, 4.4 to 15.9 mg/L, –4.8‰ to –0.2‰, –33.2‰ to 0.7‰, and –41‰ to 24‰, respectively (**Table 1**).

We found that the Type A sampling method (shallow water sampling at beaches) tended to yield lower salinity, $\delta^{18}O$, and δD values with higher variability. For example, 13 of 34 water samples collected by the Type A method had salinity values of <32.5 psu (**Table 2**), which can likely be explained by terrestrial water due to the shallow

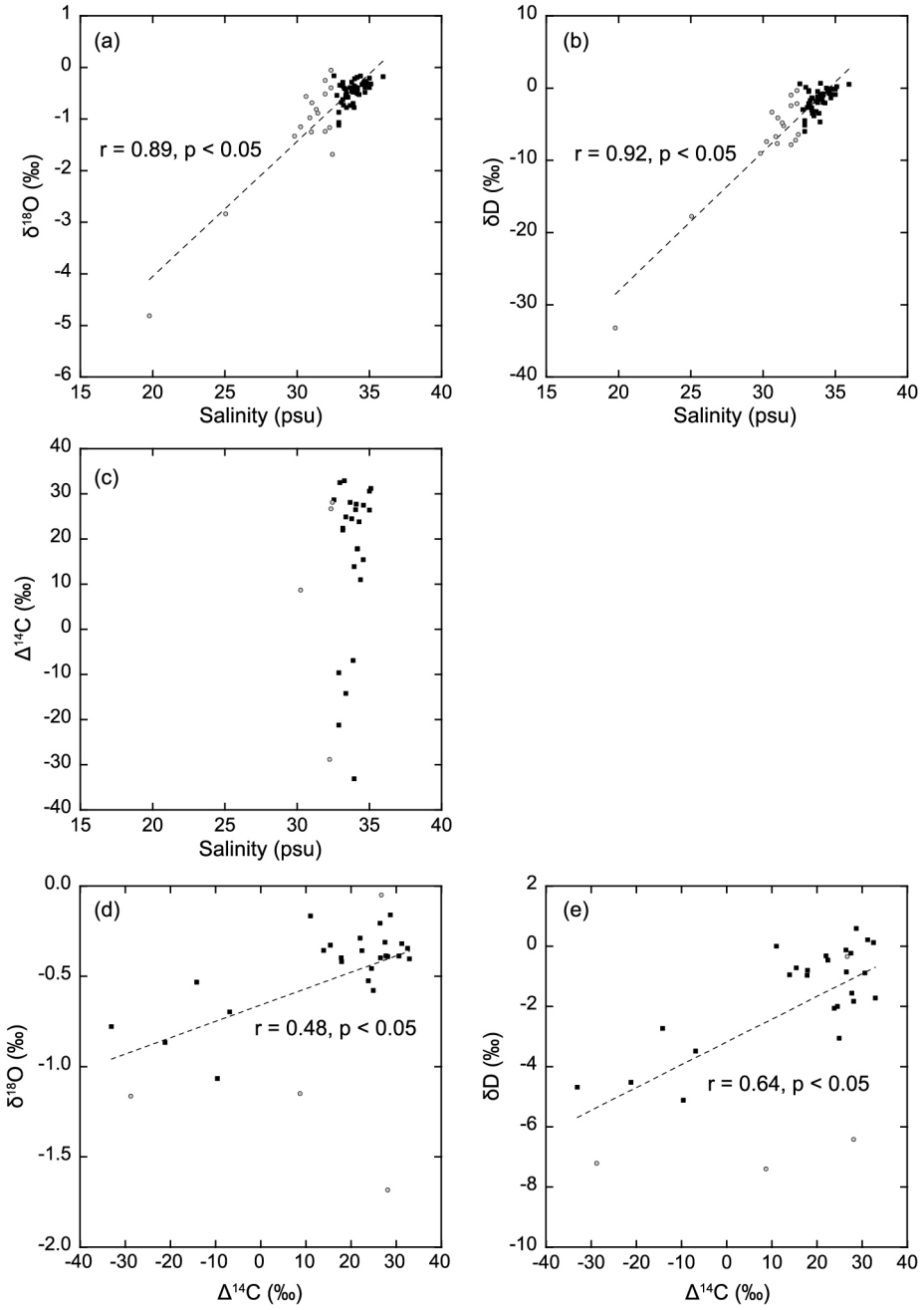

Fig. 2. Cross-plots of salinity, $\delta^{18}O$, δD, and $\Delta^{14}C$. Cross-plots of salinity versus (a) $\delta^{18}O$, (b) δD, and (c) $\Delta^{14}C$. Cross-plots of $\Delta^{14}C$ versus (d) $\delta^{18}O$ and (e) δD. Black squares/gray dots are indicate cases with salinity higher/lower than 32.5 psu. The dashed line in each figure shows the fitted linear regression line for all data points.

sampling depth. Only 4 of 30 water samples collected by the Type B method (relatively deeper water sampling at wharves) resulted in salinity values of <32.5 psu. After the removal of samples with low salinity, there were no statistically significant differences in salinity, $\delta^{18}O$, and δD values between sampling methods (p = 0.63, 0.70, and 0.90, respectively) (**Table 2**).

We observed a statistically significant positive correlation between salinity and $\delta^{18}O$ (r = 0.89, $p < 0.05$) as well as between salinity and δD (r = 0.92, $p < 0.05$) for all datapoints (**Fig. 2**, **Table 3**). When we removed water samples with low salinity (<32.5 psu), a weak correlation was still detected (r = 0.51, $p < 0.05$ for both combinations). There was no statistically significant correlation between salinity and $\Delta^{14}C$ (r = 0.24, p = 0.21, **Fig. 2**), even when low salinity data (S < 32.5 psu) were excluded from the calculation (r = 0.24, p = 0.24, **Table 3**). Similarly, there were statistically significant positive correlations between $\delta^{18}O$ and $\Delta^{14}C$ (r = 0.48, $p < 0.05$) as well as δD and $\Delta^{14}C$ (r = 0.64, $p < 0.05$) (**Fig. 2**, **Table 3**). The correlations became stronger when low salinity data were removed (r = 0.74 for the correlation between

Table 3. Summary of correlations between salinity (S), $\delta^{18}O$, δD, and $\Delta^{14}C$

All data	$\delta^{18}O$-S	δD-S	$\Delta^{14}C$-S	$\delta^{18}O$-$\Delta^{14}C$	δD-$\Delta^{14}C$
r	0.89	0.92	0.24	0.48	0.64
R^2	0.80	0.85	0.06	0.23	0.41
N	64	64	29	29	29
t	15.8	18.9	1.3	2.9	4.3
p	0.00	0.00	0.21	0.01	0.00
Statistical significance	*	*		*	*
Data with high salinity (>32.5 psu)	$\delta^{18}O$-S	δD-S	$\Delta^{14}C$-S	$\delta^{18}O$-$\Delta^{14}C$	δD-$\Delta^{14}C$
r	0.51	0.51	0.24	0.74	0.77
R^2	0.26	0.26	0.06	0.54	0.60
N	47	47	25	25	25
t	4.0	3.9	1.2	5.2	5.9
p	0.00	0.00	0.24	0.00	0.00
	*	*		*	*
Data with low salinity (<32.5 psu)	$\delta^{18}O$-S	δD-S	$\Delta^{14}C$-S	$\delta^{18}O$-$\Delta^{14}C$	δD-$\Delta^{14}C$
r	0.92	0.95	0.07	0.18	0.52
R^2	0.85	0.91	0.00	0.03	0.27
N	17	17	4	4	4
t	9.3	12.1	0.1	0.3	0.9
p	0.00	0.00	0.93	0.82	0.48
	*	*			

Asterisks indicate significant correlations ($p < 0.05$).

$\delta^{18}O$ and $\Delta^{14}C$, $r = 0.77$ for the correlation between δD and $\Delta^{14}C$) (**Table 3**). There was no consistent pattern at sites where low salinity (S < 32.5 psu) was observed (**Fig. 1**). It is unlikely that this low salinity was due to rain because the weather was sunny nearly every day during the sampling campaigns. Typically, water from the west coast of North Japan had higher $\delta^{18}O$, δD, and $\Delta^{14}C$ values than those of water from the Pacific side of Hokkaido (**Fig. 1**).

Conclusions

We reported the salinity, $\delta^{18}O$, δD, and $\Delta^{14}C$ of seawater collected from shallow water of the west coast of North Japan and all coastal areas of Hokkaido. Below, we provide rough interpretations of these new data. It is important to note that deeper analyses of the observed correlations in these geochemical data are needed.

After removing water samples with low salinity, we still detected significant correlations between salinity and both $\delta^{18}O$ and δD, suggesting that these parameters are useful for distinguishing between the Kuroshio-sourced water mass (that is, the Tsushima Warm Current and Souya Warm Current) and the Oyashio-sourced water mass. These results are consistent with the recent observation that Kuroshio has high salinity and isotopically higher $\delta^{18}O$ and δD values due to high levels of evaporation against precipitation (salinity increases and water with heavier isotopes tends to remain during evaporation at the sea surface). These findings are also consistent with the observation that the Oyashio has lower salinity and isotopically lighter $\delta^{18}O$ and δD values due to an inflow of terrestrial water from the surrounding continents into the North Pacific (terrestrial water has zero salinity and originates from rain and/or snow, which has a lighter isotopic composition than that of seawater).

Different $\Delta^{14}C$ values between the Sea of Japan coast and Pacific coast likely reflect water mass differences (i.e., Kuroshio/Oyashio waters show higher/lower values). Strong correlations between $\delta^{18}O$ and $\Delta^{14}C$ as well as δD and $\Delta^{14}C$ still exist if low salinity data are removed. It is unlikely that this relationship can be explained by terrestrial water (the DIC concentration of seawater is much higher than that of terrestrial water). The correlations are more consistent with the fact that Kuroshio, which is a part of the North Pacific subtropical gyre, has higher $\Delta^{14}C$ values because emitted bomb-^{14}C accumulated in the mixed layer of the subtropical gyre. This is also consistent with the fact that in the North Pacific, where the Oyashio Current originated, surface seawater has lower $\Delta^{14}C$ values due to the upwelling of deep water, which is less affected by bomb-^{14}C and shows greater ^{14}C decay due to long-term isolation from the atmosphere (deep-sea water circulates around the globe in ~2000 years).

Acknowledgments We thank T. Fujiki and R. Hayashi at the Okayama University of Science for their support with *in situ* seawater measurement and water sampling during the field survey. We also thank K. Seike at National Institute of Advanced Industrial Science and Technology for his advice on the field survey. We also thank M. Yoshioka at Kobe University for her support with salinity measurement of seawater in the laboratory. We also thank T. Miyajima at Atmosphere and Ocean Research Institute for help with analyzing hydrogen and oxygen isotopes of water samples. This study was financially supported by a Grants-in-Aid for Young Scientists from Foundation of Kinoshita Memorial Enterprise to K. Kubota, the Joint Research Program of the Institute for Space–Earth Environmental Research to K. Kubota, a Grants-in-Aid for field surveys from the Fukada Geological Institute to K. Sakai.

References

Bacon, S., Culkin, F., Higgs, N. and Ridout, P. (2007) IAPSO standard seawater: Definition of the uncertainty in the calibration procedure, and stability of recent batches. *J. Atmos. Oceanic Technol.* **24**, 1785–1799. https://doi.org/10.1175/JTECH2081.1

Broecker, W. S., Peng, T.-H., Östlund, G. and Stuiver, M. (1985) The distribution of bomb radiocarbon in the ocean. *J. Geophys. Res.: Oceans* **90**, 6953–6970. https://doi.org/10.1029/JC090iC04p06953

Cahyarini, S. Y., Pfeiffer, M., Nurhati, I. S., Aldrian, E., Dullo, W.-C. and Hetzinger, S. (2014) Twentieth century sea surface temperature and salinity variations at Timor inferred from paired coral $\delta^{18}O$ and Sr/Ca measurements. *J. Geophys. Res.: Oceans* **119**, 4593–4604. https://doi.org/10.1002/2013JC009594

Carreira, P. M., Marques, J. M. and Nunes, D. (2014) Source of groundwater salinity in coastline aquifers based on environmental isotopes (Portugal): Natural *vs.* human interference. A review and reinterpretation. *Appl. Geochem.* **41**, 163–175. https://doi.org/10.1016/j.apgeochem.2013.12.012

de Garidel-Thoron, T., Rosenthal, Y., Beaufort, L., Bard, E., Sonzogni, C. and Mix, A. C. (2007) A multiproxy assessment of the western equatorial Pacific hydrography during the last 30 kyr. *Paleoceanogr.* **22**, PA3204. https://doi.org/10.1029/2006PA001269

Felis, T., Suzuki, A., Kuhnert, H., Dima, M., Lohmann, G. and Kawahata, H. (2009) Subtropical coral reveals abrupt early-twentieth-century freshening in the western North Pacific Ocean. *Geology* **37**, 527–530. https://doi.org/10.1130/G25581A.1

Grossman, E. L. and Ku, T.-L. (1986) Oxygen and carbon isotopic fractionation in biogenic aragonite: Temperature effects. *Chem. Geol.: Isotope Geoscience Section* **59**, 59–74. https://doi.org/10.1016/0168-9622(86)90057-6

Hirabayashi, S., Yokoyama, Y., Suzuki, A., Miyairi, Y. and Aze, T. (2017) Multidecadal oceanographic changes in the western Pacific detected through high-resolution bomb-derived radiocarbon measurements on corals. *Geochem. Geophys. Geosyst.* **18**, 1608–1617. https://doi.org/10.1002/2017GC006854

Kodaira, T., Horikawa, K., Zhang, J. and Senju, T. (2016) Relationship between seawater oxygen isotope ratio and salinity in the Tsushima Current, the Sea of Japan. *Chikyukagaku* **50**, 263–277.

Kubota, K., Yokoyama, Y., Kawakubo, Y., Seki, A., Sakai, S., Ajithprasad, P., Maemoku, H., Osada, T. and Bhattacharya, S. K. (2015) Migration history of an ariid Indian catfish reconstructed by otolith Sr/Ca and $\delta^{18}O$ micro-analysis. *Geochem. J.* **49**, 469–480. https://doi.org/10.2343/geochemj.2.0371

Kubota, K., Shirai, K., Murakami-Sugihara, N., Seike, K., Hori, M. and Tanabe, K. (2017) Annual shell growth pattern of the Stimpson's hard clam *Mercenaria stimpsoni* as revealed by sclerochronological and oxygen stable isotope measurements. *Palaeogeogr. Palaeoclim. Palaeoecol.* **465**, 307–315. https://doi.org/10.1016/j.palaeo.2016.05.016

Kubota, K., Shirai, K., Higuchi, T. and Miyajima, T. (2018a) Oxygen and hydrogen isotope characteristics of seawater in Otsuchi Bay and meteoric water of inflowing rivers. *Coast. Mar. Sci.* **41**, 1–6.

Kubota, K., Shirai, K., Murakami-Sugihara, N., Seike, K., Tanabe, K., Minami, M. and Nakamura, T. (2018b) Bomb-^{14}C peak in the North Pacific recorded in long-lived bivalve shells (*Mercenaria stimpsoni*). *J. Geophys. Res.: Oceans* **123**, 2867–2881. https://doi.org/10.1002/2017JC013678

Kubota, K., Shirai, K., Murakami-Sugihara, N., Seike, K., Minami, M., Nakamura, T. and Tanabe, K. (2021) Evidence of mass mortality of the long-lived bivalve *Mercenaria stimpsoni* caused by a catastrophic tsunami. *Radiocarbon* **63**, 1629–1644. https://doi.org/10.1017/RDC.2021.98

Kumamoto, Y., Murata, A., Kawano, T., Watanabe, S. and Fukasawa, M. (2013) Decadal changes in bomb-produced radiocarbon in the Pacific Ocean from the 1990s to 2000s. *Radiocarbon* **55**, 1641–1650. https://doi.org/10.1017/S0033822200048554

Kuzmin, Y. V., Burr, G. S. and Jull, A. J. T. (2001) Radiocarbon reservoir correction ages in the Peter the Great Gulf, Sea of Japan, and eastern coast of the Kunashir, southern Kuriles (northwestern Pacific). *Radiocarbon* **43**, 477–481. https://doi.org/10.1017/S0033822200038364

Kuzmin, Y. V., Burr, G. S., Gorbunov, S. V., Rakov, V. A. and Razjigaeva, N. G. (2007) A tale of two seas: Reservoir age correction values (R, DR) for the Sakhalin Island (Sea of Japan and Okhotsk Sea). *Nucl. Instrum. Methods Phys. Res. B* **259**, 460–462. https://doi.org/10.1016/j.nimb.2007.01.308

Larsen, T., Yokoyama, Y. and Fernandes, R. (2018) Radiocarbon in ecology: Insights and perspectives from aquatic and terrestrial studies. *Methods Ecol. Evol.* **9**, 181–190. https://doi.org/10.1111/2041-210X.12851

LeGrande, A. N. and Schmidt, G. A. (2006) Global gridded data set of the oxygen isotopic composition in seawater. *Geophys. Res. Let.* **33**, L12604. https://doi.org/10.1029/2006GL026011.

McConnaughey T. A. (1989) ^{13}C and ^{18}O isotopic disequilibrium in biological carbonates: II. In vitro simulation of kinetic isotope effects. *Geochim. Cosmochim. Acta* **53**, 163–171. https://doi.org/10.1016/0016-7037(89)90283-4

Mitsuguchi, T., Hirota, M., Paleo Labo AMS Dating Group, Yamazaki, A., Watanabe, T. and Yamano, H. (2016) Post-bomb coral $\Delta^{14}C$ record from Iki Island, Japan: Possible evidence of oceanographic conditions on the northern East China Sea shelf. *Geo-Mar. Lett.* **36**, 371–377. https://doi.org/10.1007/s00367-016-0456-4

Mohtadi, M., Steinke, S., Lückge, A., Groeneveld, J. and Hathorne, E. C. (2010) Glacial to Holocene surface hydrography of the tropical eastern Indian Ocean. *Earth Planet. Sci. Lett.* **292**, 89–97. https://doi.org/10.1016/j.epsl.2010.01.024

Nair, I. S., Rajaveni, S. P., Schneider, M. and Elango, L. (2015) Geochemical and isotopic signatures for the identification of seawater intrusion in an alluvial aquifer. *J. Earth Syst. Sci.* **124**, 1281–1291. https://doi.org/10.1007/s12040-015-0600-y

Olsen, A., Key, R. M., van Heuven, S., Lauvset, S. K., Velo, A., Lin, X., Schirnick, C., Kozyr, A., Tanhua, T., Hoppema, M.,

Jutterström, S., Steinfeldt, R., Jeansson, E., Ishii, M., Pérez, F. F. and Suzuki, T. (2016) The Global Ocean Data Analysis Project version 2 (GLODAPv2)—An internally consistent data product for the world ocean. *Earth Syst. Sci. Data* **8**, 297–323. https://doi.org/10.5194/essd-8-297-2016

Östlund, H. G. and Stuiver, M. (1980) GEOSECS Pacific radiocarbon. *Radiocarbon* **22**, 25–53. https://doi.org/10.1017/S0033822200004707

Ota, K., Yokoyama, Y., Miyairi, Y., Hayakawa, J., Satoh, N., Fukuda, H. and Tanaka, K. (2019) Northeast Pacific seawater radiocarbon recorded in abalone shells obtained from Otsuchi Bay, Japan. *Radiocarbon* **63**, 1249–1258. https://doi.org/10.1017/RDC.2019.95

Schöne, B. R., Castro, A. D. C., Fiebig, J., Houk, S. D., Oschmann, W. and Kroncke, I. (2004) Sea surface water temperatures over the period 1884–1983 reconstructed from oxygen isotope ratios of a bivalve mollusk shell (*Arctica islandica*, southern North Sea). *Palaeogeogr. Palaeoclimatol. Palaeoecol.* **212**, 215–232. https://doi.org/10.1016/j.palaeo.2004.05.024

Stuiver, M. and Polach, H. A. (1977) Discussion reporting of ^{14}C data. *Radiocarbon* **19**, 355–363. https://doi.org/10.1017/S0033822200003672

Suess, H. E. (1953) Natural radiocarbon and the rate of exchange of CO_2 between the atmosphere and the sea. *Proc. of the Conf. on Nuclear Processes in Geological Settings* (Aldrich, L. T., ed.), 52–56, University of Chicago Press, Chicago.

Suzuki, A., Hibino, K., Iwase, A. and Kawahata, H. (2005) Intercolony variability of skeletal oxygen and carbon isotope signatures of cultured *Porites* corals: Temperature-controlled experiments. *Geochim. Cosmochim. Acta* **69**, 4453–4462. https://doi.org/10.1016/j.gca.2005.05.018

Takahashi, H. A., Minami, M., Aramaki, T., Handa, H. and Matsushita, M. (2019) Radiocarbon changes of unpoisoned water samples during long-term storage. *Nucl. Instrum. Methods Phys. Res. B* **455**, 195–200. https://doi.org/10.1016/j.nimb.2018.11.029

Takahashi, H. A., Handa, H. and Minami, M. (2021) A simple CO_2 extraction method for radiocarbon analyses of dissolved inorganic carbon in water samples without a carrier gas. *Radiocarbon* **63**, 1339–1353. https://doi.org/10.1017/RDC.2021.48

Tsunogai, S., Watanabe, S., Honda, M. and Aramaki, T. (1995) North Pacific intermediate water studied chiefly with radiocarbon. *J. Oceanogr.* **51**, 519–536. https://doi.org/10.1007/BF02270522

Voelker, A. H. L., Colman, A., Olack, G., Waniek, J. J. and Hodell, D. (2015) Oxygen and hydrogen isotope signatures of Northeast Atlantic water masses. *Deep Sea Res. II* **116**, 89–106. https://doi.org/10.1016/j.dsr2.2014.11.006

Yamano, H., Hori, K., Yamauchi, M., Yamagawa, O. and Ohmura, A. (2001) Highest-latitude coral reef at Iki Island, Japan. *Coral Reefs* **20**, 9–12. https://doi.org/10.1007/s003380100137

Yoneda, M., Kitagawa, H., van der Plicht, J., Uchida, M., Tanaka, A., Uehiro, T., Shibata, Y., Morita, M. and Ohno, T. (2000) Pre-bomb marine reservoir ages in the western North Pacific: Preliminary result on Kyoto University collection. *Nucl. Instrum. Methods Phys. Res. B* **172**, 377–381. https://doi.org/10.1016/S0168-583X(00)00361-X

Yoneda, M., Uno, H., Shibata, Y., Suzuki, R., Kumamoto, Y., Yoshida, K., Sasaki, T., Suzuki, A. and Kawahata, H. (2007) Radiocarbon marine reservoir ages in the western Pacific estimated by pre-bomb molluscan shells. *Nucl. Instrum. Methods Phys. Res. B* **259**, 432–437. https://doi.org/10.1016/j.nimb.2007.01.184